Modern Physics Letters A, Vol. 12, No. 22 (1997) 1605–1627

SINGULARITIES OF THE PARTITION FUNCTION FOR THE ISING MODEL COUPLED TO 2D QUANTUM GRAVITY

J. AMBJØRN*,‡, K. N. ANAGNOSTOPOULOS*,§ and U. MAGNEA†,+
*The Niels Bohr Institute
†NORDITA, Blegdamsvej 17, DK-2100 Copenhagen Ø, Denmark

Received 16 May 1997

We study the zeros in the complex plane of the partition function for the Ising model coupled to 2D quantum gravity for complex magnetic field and real temperature, and for complex temperature and real magnetic field, respectively. We compute the zeros by using the exact solution coming from a two-matrix model and by Monte–Carlo simulations of Ising spins on dynamical triangulations. We present evidence that the zeros form simple one-dimensional curves in the complex plane, and that the critical behaviour of the system is governed by the scaling of the distribution of the singularities near the critical point. Despite the small size of the systems studied, we can obtain a reasonable estimate of the (known) critical exponents.

1. Introduction

The understanding of the phase transition of a statistical mechanical model has long been connected to the study of its partition function zeros. This line of research was pioneered by Yang and Lee,[1] and has subsequently been pursued by many authors (for recent work see Ref. 3 and references therein). In the thermodynamic limit, the zeros of the partition function of such a system in the complex coupling space accumulate infinitely close to the critical coupling on the real axis. This defines, in the infinite volume limit, disconnected regions in the complex plane, with different analytic structure for the thermodynamic functions which describe the phases of the system.

The critical behaviour in the neighbourhood of a continuous phase transition can be extracted from the behaviour of the density of zeros near its singular points.[2,4,5] In the best-understood models, these points occur at the ends of lines on which the zeros accumulate in the infinite volume limit. Such singular points, even when they occur at non-physical values of the coupling, can be considered as ordinary critical points with distinctive critical exponents[7] (see also Ref. 8). For a physical

‡E-mail: ambjorn@nbi.dk
§E-mail: konstant@nbi.dk
+E-mail: umagnea@nbi.dk

phase transition, these singularities coincide with the (real) critical coupling of the system.

Substantial progress, also from a practical point of view, has been made by applying renormalization group arguments to the motion of zeros, thereby deriving finite size scaling relations by which the critical exponents can be computed.[6] This finite-size scaling technique applied to complex zeros has been proven powerful in numerical computations of critical exponents.

A special class of statistical systems are spin systems defined on random surfaces. In addition to being interesting systems *per se*, they have received special attention for their relation to conformal matter systems coupled to two-dimensional quantum gravity. At criticality, the spin systems are described by conformal field theories (CFT) coupled to gravity. The critical exponents of such conformal theories have been found by Knizhnik, Polyakov and Zamolodchikov (KPZ) to be simply related to the critical exponents of the same CFT defined in flat space.[9] In particular, the critical Ising model coupled to 2D gravity can be recast in the form of a $c = 1/2$ conformal field theory coupled to 2D gravity. In addition, the equivalence of the Ising model on a random surface to a Hermitian two-matrix model, discovered and studied by Kazakov and Boulatov,[10,11] renders it exactly solvable. The critical exponents were first computed this way, outside the CFT context. The system is found to have a third-order phase transition from a high temperature disordered phase to a low temperature ordered phase. The coupling between matter and the geometry of the surface is found to change the critical exponents associated to geometry only at the phase transition.

The location of the partition function zeros of the Ising model in the complex fugacity plane, the so-called Lee–Yang zeros, in the presence of gravity has been studied by Staudacher.[12] The somewhat surprising discovery that the Lee–Yang zeros lie on the unit circle in the complex fugacity plane *for each lattice size* N will be confirmed below for slightly bigger lattices than those considered in Ref. 12. As discussed by Staudacher, the Lee–Yang theorem[1] guarantees that the roots of the partition function of the Ising model on a fixed lattice $Z_{\text{flat}}(G_N)$ for a large class of not too pathological lattices G_N will lie on the unit circle, but it is not *a priori* expected that the roots of the partition function Z_N, obtained by summing the $Z_{\text{flat}}(G_N)$'s over all dynamical random lattices G_N,

$$Z_N = \sum_{\{G_N\}} Z_{\text{flat}}(G_N)\,, \tag{1.1}$$

will also be located on the unit circle. The summation in (1.1) corresponds to an integration over the additional quantum degree of freedom introduced by a fluctuating metric. The Lee–Yang theorem for this case remains unproven. *A priori* the zeros can be located on different curves or even on sets with more complicated topology, or on two-dimensional regions. The latter cases have been observed for the complex temperature zeros of 2D Ising and Potts models on hierarchical

lattices,[27] for anisotropic lattices,[28] and interestingly, also for a regular lattice made of different polygons.[29] (See also Ref. 30, where a very interesting, albeit somewhat inconclusive attempt at studying the partition function zeros of Ising spin glasses is made, and Ref. 31, where the zeros for aperiodic systems were studied.)

In this letter we use the same method as in Ref. 12 in order to compute the exact partition function for systems with up to 14 squares. We compute the Lee–Yang zeros of the partition function and confirm that they are located on the unit circle of the complex fugacity plane. We also compute the zeros of the partition function for complex temperature (Fisher zeros) and find that they move on curves in the complex temperature plane as the lattice size is varied. This indicates that in the infinite volume limit, the zeros accumulate to form dense sets on these curves. We test the scaling relations derived by Itzykson, Pearson and Zuber in the context of regular lattices[6] and extract from there some (combinations of) critical exponents. These scaling relations are based on the assumption that the spin–spin correlation length diverges at the critical point. Despite the small size of the systems studied, we find reasonable agreement with the critical exponents given in Refs. 10 and 11. This result is expected from the nontrivial fact that the matter correlation length diverges at the phase transition[13] (see Ref. 15 for an example where this is not true). This way we provide strong evidence that the phase transition is governed by the singularities of the distribution densities at $H = 0$ and β_c of the Lee–Yang and Fisher zeros respectively as is the case for the Ising model on a fixed lattice. The pattern of zeros we observe confirms the observation in Ref. 14 that no antiferromagnetic transition occurs for the Ising model on a square lattice when the spins are placed on the faces of the lattice. Using duality, we can study the pattern of the Fisher zeros of the dual model where the spins are placed on the vertices. We observe that the set of Fisher zeros maps onto itself under $\tilde{\beta} \to -\tilde{\beta}$. This indicates the existence of an antiferromagnetic transition whose critical exponents are identical to the ones of the ferromagnetic transition.[a] This confirms the results reported in Ref. 14.

One of the methods for computing complex zeros is provided by Monte–Carlo simulations and histogramming techniques. These techniques have been applied successfully to systems defined in flat space.[16,17] They have also been tried on several systems coupled to gravity (random surfaces coupled to extrinsic curvature, Potts models, 4D quantum gravity[22]) but it proved difficult to observe the partition function complex zeros. Here, we apply the method to Ising spins on dynamical triangulations,[18] and we are able to observe the zeros lying closest to the real axis for a range of lattice sizes with up to 256 vertices. In general, it was easier to find the Lee–Yang zeros than the Fisher zeros. In the latter, we were able to locate only the first zero for any given lattice size. After determining the position of the zeros as a function of lattice size, we test their scaling and the critical exponents computed are in reasonable agreement with their exactly known values.

[a]We thank D. Johnston for pointing this out.

In Sec. 2 we define our model and review the expected scaling behaviour of the zeros on the assumption of a diverging matter correlation length. In Sec. 3 we describe in detail the methods we use in order to compute the zeros, and in Sec. 4 we test their finite size scaling behaviour. Section 5 contains some concluding remarks.

2. The Model

We will study one Ising model on a dynamical square or triangular lattice. In the former, the spins are located on the N faces (squares) of the lattice, in the latter on the N_v vertices. The partition function for a fixed lattice G_N is given by

$$Z_{\text{flat}}(G_N, \beta, H) = \sum_{\{\sigma\}} e^{\beta \sum_{\langle i,j \rangle} \sigma_i \sigma_j + H \sum_i \sigma_i}, \tag{2.2}$$

and the partition function $Z(N, \beta, H)$ for the model coupled to quantum gravity is obtained by summing $Z_{\text{flat}}(G_N, \beta, H)$ over all lattices G_N with spherical topology and N faces

$$Z(N, \beta, H) = \sum_{\{G_N\}} Z_{\text{flat}}(G_N, \beta, H)\,. \tag{2.3}$$

In Eq. (2.2) $\sum_{\langle i,j \rangle}$ denotes a sum over the neighbouring pairs of faces (in the case of a square lattice) or vertices (in the case of a triangular lattice) of G_N. $\sum_{\{\sigma\}}$ denotes the sum over all the possible spin configurations, β is the inverse temperature and H the magnetic field. $\sum_{\{G_N\}}$ is the discrete analog of summing over all possible metrics up to diffeomorphisms on a spherical surface of fixed volume, since G_N defines a metric on the discretized surface if we define each link to have the same fixed length. The class of lattices we consider includes degenerate ones which have double links and vertices of order one.

The system (2.3) undergoes a third-order phase transition whose universal properties are independent of the microscopic details of the lattice.[10,11] For the square lattice, the critical inverse temperature is given by $\beta_c = \ln 2 \approx 0.693\,147\,18$, and for the triangular lattice, $\beta_c = \frac{1}{2} \ln[(13 + \sqrt{7})/(14 - \sqrt{7})] \approx 0.160\,303\,70$.[14] The critical exponents are given by[11]

$$\beta = 1/2\,, \tag{2.4}$$

$$\gamma = 2\,, \tag{2.5}$$

$$\delta = 5\,, \tag{2.6}$$

$$\nu d_{\text{H}} = 3\,, \tag{2.7}$$

which are defined in the usual way by the behaviour of the magnetization $M \sim |\beta - \beta_c|^{\beta}$, $M \sim H^{1/\delta}$ and the magnetic susceptibility $\chi_M \sim |\beta - \beta_c|^{-\gamma}$ in the critical region. ν is the spin–spin correlation length exponent $\xi \sim |\beta - \beta_c|^{-\nu}$, and d_{H} denotes the Hausdorff dimension of space.

For a given lattice G_N, the partition function (2.2) can be written (up to a multiplicative constant) as a polynomial

$$Z_{\text{flat}}(G_N, \beta, H) = \sum_{m=0}^{N} \sum_{n=0}^{N_l} C_{mn} y^m c^n \,, \tag{2.8}$$

where $c = e^{-2\beta}$, $y = e^{-2H}$, N is the number of faces in G_N (when we put the spins on the faces) and N_l the number of links. y is called the fugacity. In the following we will also use the notation $u = e^{-4\beta}$ and $K = u - u_c$.

Equation (2.8) is a polynomial in two variables, and its analytic structure is entirely determined by its zeros in the complex plane. If we fix the temperature β, $Z_{\text{flat}}(G_N, \beta, H)$ is a polynomial in y and its zeros were shown by Yang and Lee[1] to lie on the unit circle in the complex fugacity plane. We expect the theorem to be true for a large class of (not too pathological) lattices G_N. Then one can write the free energy of the system as

$$F_{\text{flat}}(G_N, \beta, y) = -\ln \prod_{k=0}^{N} (y - y_k(\beta)) \,, \tag{2.9}$$

where a factor β has been absorbed into $F_{\text{flat}}(G_N, \beta, y)$ and an additive constant has been suppressed ($y \equiv e^{-2H}$). Here $y_k(\beta)$ are the zeros of $Z_{\text{flat}}(G_N, \beta, H)$ in the y plane, called the Lee–Yang zeros. In the thermodynamic limit these zeros form dense sets on lines, which are Stokes lines for $F_{\text{flat}}(G_\infty, \beta, y)$. All the relevant information is then encoded in the density of zeros $\rho_{\text{YL}}(\beta, \theta)(H = i\theta)$. The free energy per spin in the limit of infinite volume $N \to \infty$ is then given by

$$F_{\text{flat}}(G_\infty, \beta, y) = -\int_{-\pi}^{\pi} d\theta \, \rho_{\text{YL}}(\beta, \theta) \ln(y - e^{-2i\theta}) \,. \tag{2.10}$$

Here -2θ denotes the polar angle on the unit circle of the partition function zero in the complex y-plane. This notation is motivated by the Lee–Yang theorem. The singularities of the partition function are expected to occur at the ends of the lines on which the partition function zeros condensed. In the case of (2.2), in the high temperature phase the zeros form a gap $\theta_0 > 0$ such that $\rho_{\text{YL}}(\beta, \theta) = 0$ for $|\theta| < \theta_0$. The points $y_0 = e^{\pm 2i\theta_0}$ are the Lee–Yang edge singularities and they can be regarded as conventional critical points.[7] The (only) characteristic critical exponent σ is

$$\rho_{\text{YL}}(\beta, \theta) \sim (\theta - \theta_0)^\sigma \,, \tag{2.11}$$

which implies that $M \sim (\theta - \theta_0)^\sigma$. In Ref. 26 it was shown that $\sigma = -1/6$ in two dimensions.

As we approach the critical temperature from above, the gap closes ($\theta_0 \to 0$) and the zeros pinch the real axis at $y = 1$. This signals the onset of the phase transition, since the partition function has different analytic behaviour in the two disconnected parts of the y-plane. The information on the universal scaling of the

partition function is given by the scaling of $\rho_{\rm YL}(\beta,\theta)$ near $\theta = 0$. At $\beta = \beta_{\rm c}$, $\theta_0 = 0$ and if we define $M \sim H^{1/\delta}$ we obtain

$$\rho_{\rm YL}(\beta_{\rm c},\theta) \sim \theta^{1/\delta}\,. \tag{2.12}$$

Other critical exponents can be derived from scaling relations discussed in Ref. 6 and later in this section. For a finite system the zeros are never on the positive real axis since C_{mn} is positive and $c > 0$ for real β in Eq. (2.8). When the system is critical, i.e. when the correlation length $\xi \sim L$ (L is the linear size of the system), the zeros approach the real axis infinitely close as $L \to \infty$ and one can apply finite size scaling in order to extract critical exponents.

If we fix y in Eq. (2.8), we obtain a polynomial of order N_l in c. Its zeros in the c-plane are the so-called Fisher zeros.[2] For many systems the Fisher zeros are located on curves C, but this is not necessarily true in general. For the 2D (zero-field) Ising model on a square lattice, these curves C are two intersecting circles (both in the c-plane and in the $\tanh(\beta)$ plane). One of the curves intersects the real positive axis at the physical critical point. Similarly to the case of Lee–Yang zeros, the Fisher zeros condense on these two curves in the thermodynamic limit and the free energy per spin is given, in this limit, by their density $\rho_F(\beta,H)$:

$$F_{\rm flat}(G_\infty,\beta,H) = -\int_C d\beta' \rho_F(\beta',H)\ln(c(\beta) - e^{-2\beta'})\,, \tag{2.13}$$

where β' is a complex number. Near the critical temperature and at $H = 0$,

$$\rho_F(\beta,H=0) \sim |\beta - \beta_{\rm c}|^{-\alpha+1}\,, \tag{2.14}$$

which implies that $F_{\rm flat}(G_\infty,\beta,H=0) \sim |\beta-\beta_{\rm c}|^{-\alpha+2}$. Therefore α is the specific heat exponent.

The possibility of extracting scaling exponents from the study of complex zeros of the partition function relies on their scaling behaviour under the renormalization group.[6] Applying finite size scaling is a convenient method often used in numerical simulations. Simple scaling arguments[6] give the position of the jth Lee–Yang zero as

$$H_j^2 N^{2\beta\delta/(\nu d_{\rm H})} = f_j(KN^{1/(\nu d_{\rm H})})\,, \tag{2.15}$$

where we have substituted $N^{1/d_{\rm H}}$ for the linear size L of the system (N is the volume and $d_{\rm H}$ is the Hausdorff dimension). f_j is an analytic function and the Lee–Yang theorem implies that $f_j(0) < 0$. If we invert the above relation we obtain the positions of the Fisher zeros. Hence we can deduce that the jth Lee–Yang zero will scale as

$$H_j \sim N^{-\beta\delta/(\nu d_{\rm H})}\,, \tag{2.16}$$

and the jth Fisher zero as

$$K_j \sim N^{-1/(\nu d_{\mathrm{H}})} . \tag{2.17}$$

The gap of the Lee–Yang edge singularity will scale as

$$H_0^2 \sim -CK^{2\beta\delta} , \tag{2.18}$$

where $C > 0$ and $H_0 \equiv i\theta_0$. Conversely, in the scaling region the dependence of the jth Fisher zero on the value of the (real) magnetic field will be

$$K_j \sim e^{\frac{i\pi}{2\beta\delta}} \left(\frac{H}{\sqrt{C}}\right)^{1/(\beta\delta)} . \tag{2.19}$$

Equation (2.19) implies that the trajectories of the motion of the Fisher zeros in the K plane with varying real nonzero H will form an angle

$$\psi = \frac{\pi}{2\beta\delta} \tag{2.20}$$

with the real K-axis. Using Eq. (2.15) a stronger scaling relation can be derived:

$$H_j^2 (N/j)^{2\delta/(\delta+1)} = F\left(K(N/j)^{1/(\nu d_{\mathrm{H}})}\right) , \tag{2.21}$$

where F is a universal analytic scaling function such that $F(0) < 0$, H_j is the jth Lee–Yang zero. Similarly

$$K_j = \left(\frac{j}{N}\right)^{1/(\nu d_{\mathrm{H}})} F^{-1}(0) , \tag{2.22}$$

where K_j is the jth Fisher zero.

In Ref. 13, we provided evidence that there exists a divergent correlation length associated to matter fields coupled to gravity in the range of central charge $0 < c < 1$. Based on these results, we expect that the observed zeros, for large enough lattices, might show a behaviour compatible with the scaling hypothesis. It is the main purpose of this work to provide evidence that this is indeed the case.

3. Computation of Complex Zeros

Our computation of Lee–Yang zeros (real β, complex H) and Fisher zeros (real H, complex β) of the partition function $Z(N, \beta, H)$ was done using exact results from matrix models and Monte–Carlo multihistogramming techniques. We describe these methods in this section.

3.1. *Exact determination of partition functions*

The exact solution of the Ising model on a square dynamical lattice came from solving the planar limit of the two-matrix model defined in Refs. 10 and 11. It was noticed that in this limit the free energy of the model

$$F(n,g,\beta,H) = \ln\left(\int d^{n^2}\phi_1 d^{n^2}\phi_2 \exp\left[-\mathrm{Tr}(\phi_1^2+\phi_2^2-2c\phi_1^2\phi_2^2+(ge^H/n)\phi_1^4 + (ge^{-H}/n)\phi_2^4)\right]\right), \tag{3.23}$$

where $\phi_{1,2}$ are $n\times n$ Hermitian matrices, equals the grand canonical partition function $Z(g,\beta,H)$ for the Ising model coupled to gravity:

$$\lim_{n\to\infty}\frac{1}{n^2}F(n,g,\beta,H) = Z(g,\beta,H) \equiv \sum_{N=1}^{\infty}\tilde{c}^N Z(N,\beta,H), \tag{3.24}$$

where $\tilde{c} = -4gc/(1-c^2)^2$. The solution for $Z(g,\beta,H)$ is given by[10,11]

$$Z(g,\beta,H) = \frac{1}{2}\ln\left[\frac{z(g)}{g}\right] + \frac{1}{2g^2}\int_0^{z(g)}\frac{dz'}{z'}g(z')^2 - \frac{1}{g}\int_0^{z(g)}\frac{dz'}{z'}g(z'), \tag{3.25}$$

where

$$g(z) = \frac{1}{9}c^2z^3 + \frac{1}{3}z\left[\frac{1}{(1-z)^2} - c^2 + \frac{2z(\cosh H - 1)}{(1-z^2)^2}\right]. \tag{3.26}$$

Using Eqs. (3.25) and (3.26) we can expand $Z(g,\beta,H)$ in powers of g and read off the coefficients $Z(N,\beta,H)$ (corresponding to lattice size with N squares) in Eq. (3.24).

We have done this using the symbolic manipulation program *Mathematica* for $N \le 14$. We obtain

$$Z(N,\beta,H) = c^{-N}y^{-\frac{N}{2}}\sum_{m=0}^{N}\sum_{n=0}^{4\left[\frac{N}{2}\right]} D_{mn}\, y^m c^n, \tag{3.27}$$

where $[\,.\,]$ denotes integral part. The same calculation for $N \le 6$ was done in Ref. 12 and our results are in complete agreement. Then the roots of $Z(N,\beta,H)$ for either fixed β or fixed H were computed numerically. Note that, apart from a trivial multiplicative factor, the partition function is a polynomial and has a finite number of zeros in the complex c and y planes.

As already discussed above, and in Ref. 12 for $N \le 6$, the Lee–Yang zeros can be seen, somewhat surprisingly, to lie on the unit circle in the complex y-plane. No Lee–Yang theorem has so far been proven for the partition function of the dynamical lattice. Figure 1 shows the results for lattice sizes $8 \le N \le 14$, at the (bulk) critical temperature. This figure clearly shows that the zero closest to the real positive axis approaches the point $y = 1$ as we increase the lattice size, indicating a vanishing gap at β_c as $N \to \infty$. We will study this approach quantitatively using finite size scaling in the next section.

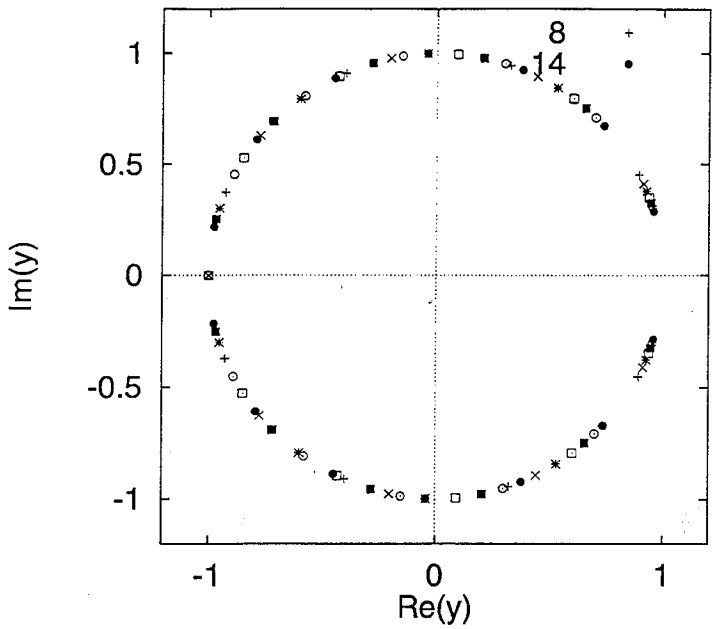

Fig. 1. Lee–Yang zeros in the complex fugacity ($y = e^{-2H}$) plane for the Ising model on square dynamical lattices of varying sizes $N = 8(+)$, $9(\times)$, $11(\square)$, $12(\blacksquare)$, $13(\circ)$, $14(\bullet)$ at the bulk critical temperature.

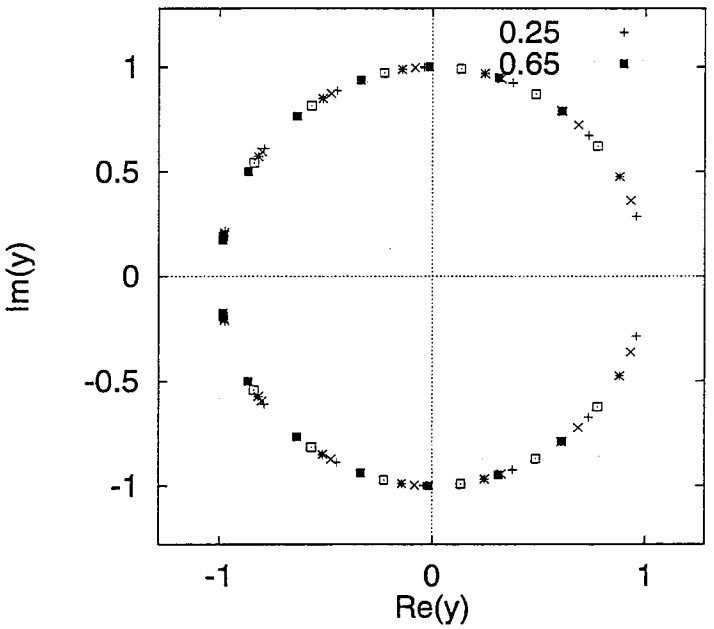

Fig. 2. Lee–Yang zeros in the complex fugacity plane for a square lattice with $N = 14$ at the critical point ($c_c = e^{-2\beta_c} = 0.25(+)$) and in the hot phase ($c = 0.35(\times)$, $0.45(*)$, $0.55(\square)$, $0.65(\blacksquare)$).

In Fig. 2 we show the motion of Lee–Yang zeros with varying β for the $N = 14$ lattice as we approach β_c from the hot phase. The zeros close up towards the point $y = 1$ ($H = 0$) on the real axis, reflecting the expected vanishing of the gap in $\rho_{YL}(\beta, \theta)$ for $\beta \to \beta_c$ in the infinite volume limit.

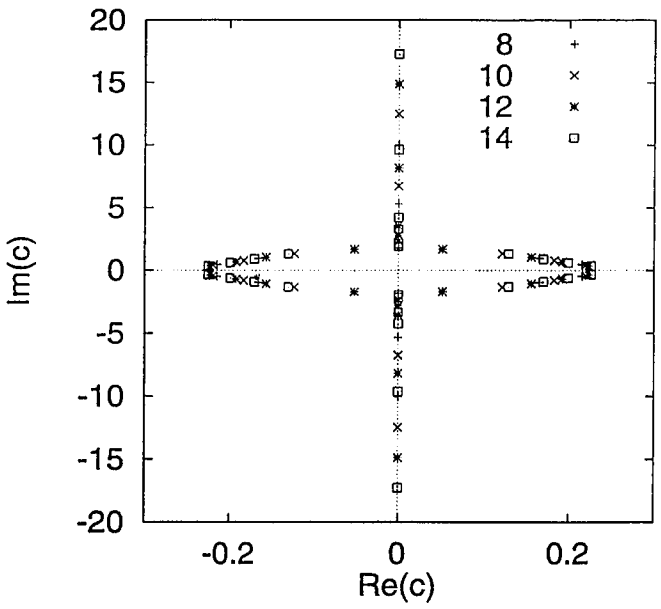

(a)

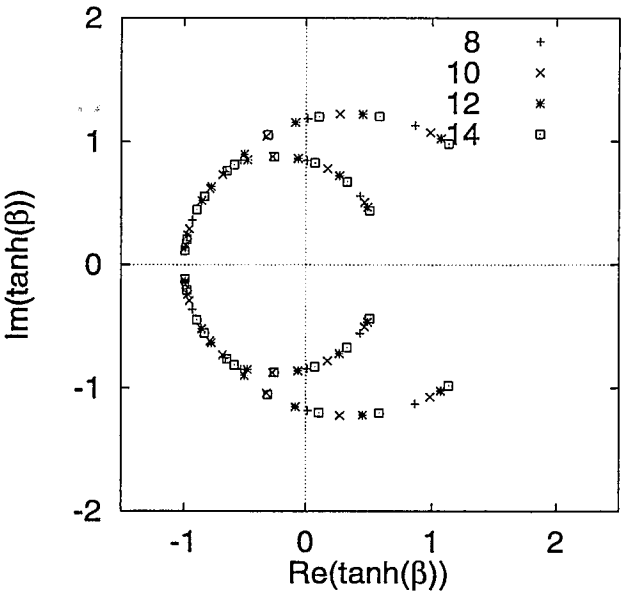

(b)

Fig. 3. Fisher zeros in the complex c-plane ($c = e^{-2\beta}$) for the Ising model with spins on the faces of square dynamical lattices of varying sizes ($N = 8, 10, 12, 14$) at $H = 0$. The zeros move on arcs and on the imaginary axis. The zeros flow towards $\pm i\infty$ on the Im(c) axis, and towards the critical points $c = (1/4, 0)$ and $c = (-1/4, 0)$ on the real axis as the thermodynamic limit is approached. The physical critical point is $c = 1/4$. (b) The trajectories in (a) shown in the complex $\tanh(\beta)$ plane. Recalling the duality relation $\tilde{c} = \tanh(\beta)$, this corresponds to (a) for the model with spins on the vertices (with $\tilde{c}$ related to the dual inverse temperature $\tilde{\beta}$ by $\tilde{c} = e^{-2\tilde{\beta}}$). The zeros approach the points $(-1, 0)$, $(3/5, 0)$ and $(5/3, 0)$ as $N \to \infty$. The point $\tilde{c} = 3/5$ corresponds to the ferromagnetic and the point $\tilde{c} = 5/3$ to the antiferromagnetic transition of the model. The zeros are mapped onto each other under $\tilde{c} \to 1/\tilde{c}$.

We also note from Figs. 3 and 4 that the Fisher zeros form curves in the complex plane. In Fig. 3a we display the approach of the Fisher zeros for $H = 0$ to the (physical and unphysical) critical points on the real axis, $c = \pm 1/4$ for increasing lattice size. There are also Fisher zeros on the imaginary axis, which flow to $c = \pm i\infty$. In Fig. 3b we show the same curves mapped onto the $\tilde{c}$-plane, where the tilde refers to the *dual* spin model. The usual duality relation is given by $\tilde{c} = \tanh(\beta)$. We note that our model is not self-dual, so the critical point $c_c = 1/4$ is different from the dual critical point $\tilde{c}_c = 3/5$. Figure 3b suggests the existence of an antiferromagnetic phase transition for the Ising model on a square lattice with spins placed on the vertices.[14] It happens at $\tilde{c}_c^{(af)} = 5/3$. This corresponds to the unphysical value of $c = -1/4$, reflecting the fact that no antiferromagnetic transition occurs for the Ising model coupled to 2D gravity on a square lattice with spins placed on the faces. We notice that the zeros in the $\tilde{c}$-plane are mapped *exactly* onto each other under the transformation $\tilde{c} \to 1/\tilde{c}$. This implies that the critical exponents of the antiferromagnetic transition are identical to the ones of the ferromagnetic transition, as was noted in Ref. 14.

Figure 4a shows the flow of Fisher zeros with varying magnetic field H for a fixed lattice size $N = 14$. The zeros on the arcs flow away from the imaginary axis as H increases, while the zeros on the imaginary axis again appear to move towards $c = \pm i\infty$ (note that these points are mapped onto $\tilde{c} = (-1, 0)$ in Fig. 4c). For $H = 0$ the zeros should pinch the real axis like in Fig. 3, but for $H \neq 0$ they seem to

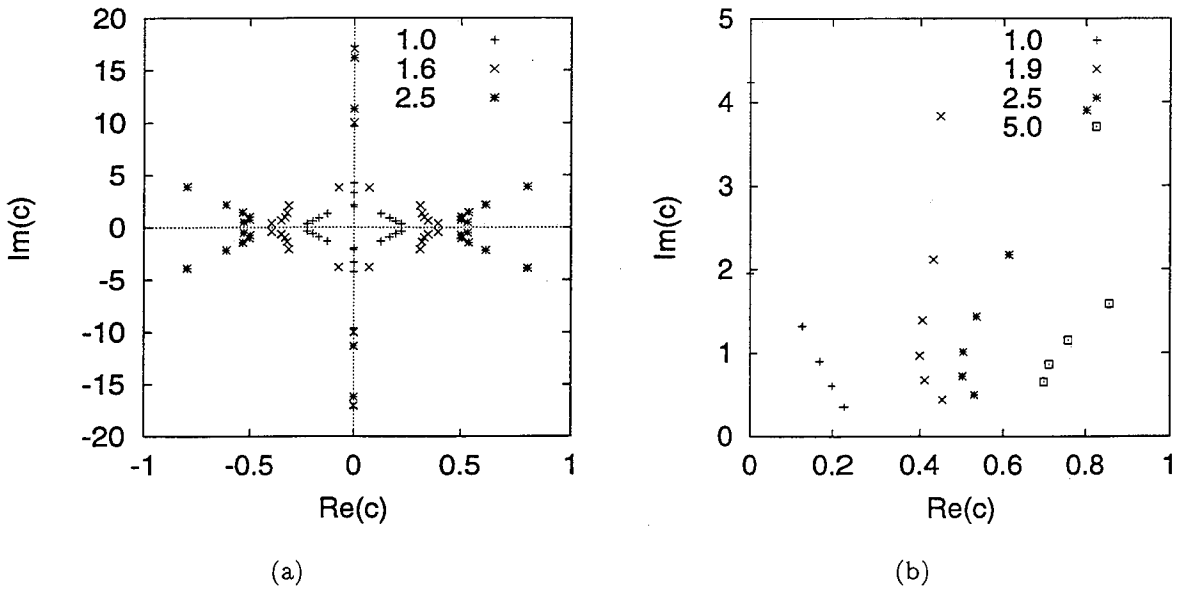

Fig. 4. (a) Fisher zeros in the complex c-plane for a square dynamical lattice of size $N = 14$ and at varying magnetic fields ($y = e^{-2H} = 1.0,\ 1.6,\ 2.5$). For zero magnetic field, the zeros with $\mathrm{Re}(c) > 0$ end in the vicinity of the physical critical point $c = (1/4, 0)$. (b) The first quadrant in (a) shown magnified for several values of the fugacity $y = 1.0,\ 1.9,\ 2.5,\ 5.0$. (c) The trajectories in (a) shown in the complex $\tilde{c}$-plane for zero and nonzero magnetic fields. The fugacity takes the values $y = 1.0,\ 1.3,\ 1.6,\ 1.9,\ 2.5$ and $N = 14$.

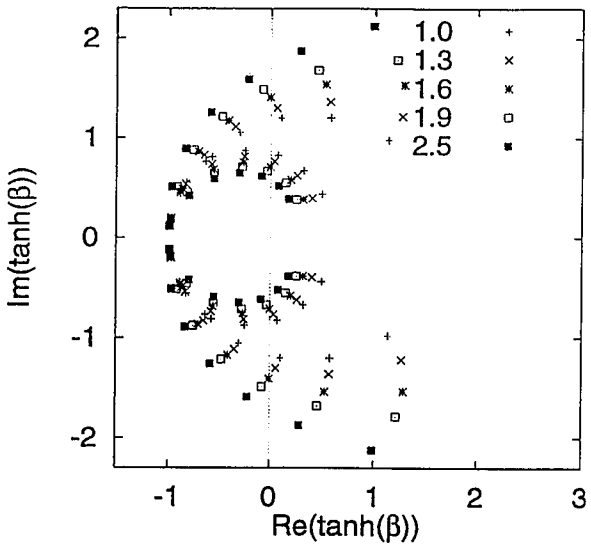

(c)

Fig. 4. (*Continued*)

avoid the real axis. This is compatible with the absence of a phase transition in the presence of a symmetry breaking field. In Fig. 4c we show the same flow in the $\tilde{c}$-plane.

3.2. *Multihistogramming of Monte–Carlo data*

For systems with more than a few spins, the study of complex zeros must rely on numerical methods. Monte–Carlo methods are very powerful in studying a system using the full Hamiltonian. They can be used to study singularities of observables in the complex plane as was done in the pioneering work, Ref. 16. With the development of (single) histogramming techniques the partition function could be calculated for a continuous region in the coupling space and its zeros determined in the complex plane.[17] Using multihistogramming,[20] where Monte–Carlo data taken at different couplings are combined optimally, a more accurate determination of the partition function is possible over a wide range of couplings. This method for computing complex zeros was first used in Ref. 21. Here we provide a brief description of the method, in order to describe the procedure we followed. For details see Ref. 32.

The Monte–Carlo updating of the triangulations was performed by the so-called flip algorithm and the spins were updated using a standard cluster algorithm. One updating sweep of the lattice consisted of approximately N_l *accepted* flips where N_l is the number of links of the triangulated surface. After a sweep of the lattice we updated the spin system. All this is by now standard and we refer to Refs. 18 and 19 for details. We use the high quality random number generator RANLUX[34] whose excellent statistical properties are due to its close relation to the Kolmogorov K-system originally proposed by Savvidy *et al.*[33]

The lattice sizes that we simulated ranged from 32 to 256 vertices. In order to minimize finite size effects, we took the spins to be on the vertices of the triangulations and included degenerate triangulations with double links and vertices of order one.[19] First we made a rough map of the partition function. Since the partition function is invariant under $\beta \to \beta + ik\pi/2$ and $H \to H + ik\pi/2$, it is not necessary to calculate $|Z_N|^2$ for $\mathrm{Im}(\beta) > \pi/2$ or $\mathrm{Im}(H) > \pi/2$. In our calculation we took H to be purely imaginary. Then we scanned the region where we expected to see the first zeros, and ultimately we took a denser grid of measurements around the points where the partition function touched zero within errors. For the largest lattice, 55 million sweeps were performed at each of 11 values β_k around the location of the zeros, in order to get a sufficiently accurate determination of the partition function in this region. For each β_k we computed energy and magnetization histograms $h^k(E, M)$, where E is the total energy and M the (absolute value of the) magnetization, from which one can obtain an approximate estimate of the density of states:

$$\rho(E, M) = \sum_k w_k(E)\rho_k(E, M) = \sum_k w_k(E) h^k(E, M) e^{\beta_k E} . \tag{3.28}$$

The coefficients $w_k(E)$ are the appropriate weights for an optimal determination of $\rho(E, M)$

$$w_k(E, M) = \frac{1}{\sum_l \frac{n^l}{n^k}\frac{\tau_k}{\tau_l} \exp((\beta_k - \beta_l)E + F_l)} , \tag{3.29}$$

where $n^{k,l}$ is the number of measurements at $\beta_{k,l}$, and $\tau_{k,l}$ the respective autocorrelation times. F_l is the free energy at β_l, determined self-consistently from

$$e^{-F_l} \equiv Z(\beta_l) = \sum_{E,M,k} \frac{h^k(E, M)}{\sum_j \frac{n^j}{n^k}\frac{\tau_k}{\tau_j} \exp((\beta_l - \beta_j)E + F_j)} . \tag{3.30}$$

Then the partition function $Z(\beta)$ and any observable $\langle \mathcal{O}(E, M)\rangle_\beta$ for real β is given by:

$$Z(\beta) = \sum_{E,M} \rho(E, M) e^{-\beta E} , \tag{3.31}$$

$$\langle \mathcal{O}(E, M)\rangle_\beta = \frac{1}{Z(\beta)} \sum_{E,M} \mathcal{O}(E, M)\rho(E, M) e^{-\beta E} . \tag{3.32}$$

Lee–Yang zeros are computed from the minima of

$$\frac{Z(\beta, H)}{Z(\beta)} = \langle \cos(\mathrm{Im}(H)M)\rangle - i\langle \sin(\mathrm{Im}(H)M)\rangle \tag{3.33}$$

for real β and imaginary H and $Z(\beta) \equiv Z(\beta, 0)$. The Fisher zeros were computed from the minima of

$$\frac{Z(\beta)}{Z(\mathrm{Re}\,\beta)} = \langle \cos(\mathrm{Im}(\beta)E) \rangle - i \langle \sin(\mathrm{Im}(\beta)E) \rangle \tag{3.34}$$

for complex values of β and $H = 0$. The errors in the partition function and in the position of the complex zeros were computed by a standard binning procedure.

Tables 1 and 2 contain our results for the zeros. We first checked that multihistogramming was working quite well with our data by looking at multihistograms of the specific heat and susceptibility. It was relatively easy to observe the first few Lee–Yang zeros. For Fisher zeros the computation was harder and in a similar way we could only clearly observe the zero closest to the real β-axis. Delicate cancellations in $|Z|^2$ between contributions from the two terms in Eq. (3.34) make the zeros located further away from the real axis disappear in the statistical noise. This sets limitations to the size of the surface on which we were able to observe Fisher zeros.

Table 1. Lee–Yang zeros observed using multihistogramming.

N_v	$\beta \pm \Delta\beta$	$\mathrm{Im}(H) \pm \Delta\,\mathrm{Im}(H)$
64	0.1718 ± 0.0005	0.203 ± 0.003
96	0.1666 ± 0.0004	0.1484 ± 0.0002
	0.2114 ± 0.0004	0.2454 ± 0.0004
128	0.1643 ± 0.0014	0.1182 ± 0.0005
	0.2037 ± 0.0012	0.195 ± 0.005
	0.2386 ± 0.0018	0.260 ± 0.003
256	0.1596 ± 0.0010	0.069 ± 0.003
	0.1850 ± 0.0017	0.112 ± 0.004
	0.2069 ± 0.0009	0.148 ± 0.005
	0.2262 ± 0.0009	0.185 ± 0.001
	0.2497 ± 0.0034	0.175 ± 0.005

Table 2. Fisher zeros observed using multihistogramming.

N_v	$\mathrm{Re}(\beta) \pm \Delta\,\mathrm{Re}(\beta)$	$\mathrm{Im}(\beta) \pm \Delta\,\mathrm{Im}(\beta)$
32	0.1428 ± 0.0016	0.1773 ± 0.0005
64	0.1481 ± 0.0049	0.1348 ± 0.0022
96	0.1533 ± 0.0021	0.1121 ± 0.0034
128	0.1556 ± 0.0300	0.1030 ± 0.0050
256	0.1527 ± 0.0035	0.0788 ± 0.0047

4. Verification of Scaling Relations

In this section we discuss the extent to which the scaling relations Eqs. (2.15)–(2.22) hold for the Ising model on a *dynamical* lattice. There is no *a priori* reason to expect these relations to hold. As discussed earlier, for the fixed lattice, their validity is due to the divergence of the spin–spin correlation length in the critical region. For the Ising model on a dynamical lattice, we expect the correlation length associated to *geometry* fluctuations to diverge,[23–25] but the same need not necessarily be true for the spin–spin correlation length even at a continuous transition.[15] Recently, however, numerical evidence indicated that this is indeed the case, and that the system behaves as an ordinary statistical system near a third-order phase transition.[13]

Numerical simulations[13,23,24] further indicate that the Hausdorff dimension of the system is very close to 4. From this value we can estimate the linear size $L \equiv N^{1/d_H}$ of the systems that we are studying and find that it is indeed quite small. In spite of substantial finite size effects, our results will provide evidence that the scaling relations are indeed satisfied by the motion of the complex zeros with varying lattice size, couplings, or the order of the zero. We can, in general, observe reasonable agreement with the known critical exponents (we will refer to these as the KPZ exponents). In the cases where a deviation from the expected value is observed, we can observe an asymptotic approach to this value with increasing lattice size.

4.1. *Zeros of the exact partition functions for small square lattices*

At $K = 0$ and large enough N, Eq. (2.16) implies

$$\ln|H_j| = -\frac{\beta\delta}{\nu d_H}\ln(N) + C_j\,. \tag{4.35}$$

The slope on a log–log plot of H_j vs N is expected to take the value

$$-\frac{\beta\delta}{\nu d_H} = -5/6 = -0.8333\ldots \tag{4.36}$$

for all j. Figure 5 and Table 3 show our results for the first three Lee–Yang zeros. The extracted exponent combination is in reasonable agreement with the KPZ exponents, especially for the first zero. The errors reported in Table 2 are not true statistical errors (which are meaningless in this case). They are computed from the standard formula giving least squares linear fit errors and in this case they are simply a measure of the systematic deviation of the points from a straight line. We will follow this practice for our fits throughout this section.

Equation (2.22) implies

$$\ln|K_j| \equiv \ln|u_j - u_c| = \frac{1}{\nu d_H}\ln\left(\frac{j}{N}\right) + C\,. \tag{4.37}$$

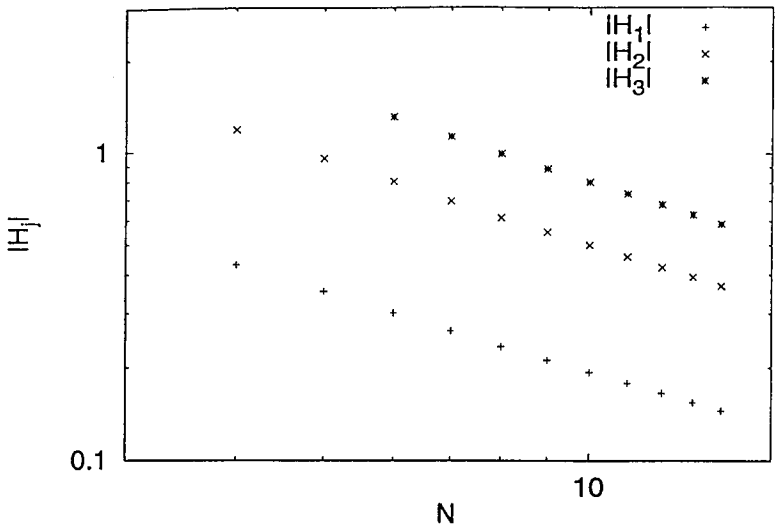

Fig. 5. Scaling of the first three Lee–Yang zeros for the Ising model on square dynamical lattices of size N (j labels the zero). The slopes are expected to be given by the exponent combination $-\beta\delta/(\nu d_{\rm H}) = -5/6$. The fitted slopes are given in Table 3.

Table 3. Predictions for the combination of critical exponents $-\frac{\beta\delta}{\nu d_{\rm H}}$ from scaling of the first three Lee–Yang zeros of exactly known partition functions Z_N.

j	Slope
1	-0.871 ± 0.002
2	-0.935 ± 0.002
3	-0.951 ± 0.002

Similarly, since $|K_j| \propto |\beta_j - \beta_{\rm c}| + O(|\beta_j - \beta_{\rm c}|^2)$, we would expect that

$$\ln|\beta_j - \beta_{\rm c}| = \frac{1}{\nu d_{\rm H}} \ln\left(\frac{j}{N}\right) + C\,, \tag{4.38}$$

where the slope should be given by

$$\frac{1}{\nu d_{\rm H}} = \frac{1}{3}\,, \tag{4.39}$$

and the constant C should be independent of j. Table 4 shows the results of fits to Eq. (4.38), and similar fits with N replaced by N_v, the number of vertices of the lattice. The corresponding fits using the scaling variable K did not yield straight lines in a log–log plot, as can be seen from Fig. 6. In this figure, we have plotted $|K_1|$ (lower curve) resp. $|\beta_1 - \beta_{\rm c}|$ (upper curve) vs N on a logarithmic scale. The difference between the scaling behaviour of the two different scaling variables (which are expected to be identical for very large systems), shows that we are not deep in the scaling region and that finite size effects are important for the system sizes that we consider. The same must be said about the difference between the slopes

Table 4. Slopes and intercepts from the fits to Eq. (4.38). The theoretical value for the slope is $\frac{1}{\nu d_H} = 1/3$. The dependence of the slope and of C on j indicates finite size effects, as does the difference between N and N_v. n is the number of degrees of freedom in the fits.

Quantity fitted	j	Slope	C	n
$\ln\lvert\beta - \beta_c\rvert$ vs $\ln(j/N)$	1	0.327 ± 0.001	0.295 ± 0.002	8
	2	0.377 ± 0.002	0.490 ± 0.005	4
$\ln\lvert\beta - \beta_c\rvert$ vs $\ln(j/N_v)$	1	0.383 ± 0.002	0.492 ± 0.006	6
	2	0.438 ± 0.004	0.667 ± 0.009	4

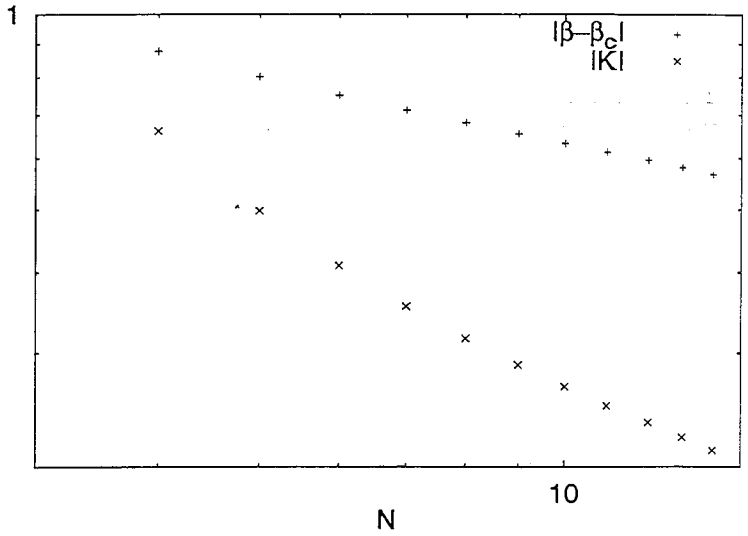

Fig. 6. Illustration of the scaling relation $|K| \propto N^{-1/(\nu d_H)}$ for the first Fisher zero at $H = 0$. Due to finite size effects, the curve for $|K|$ is not a straight line. On the other hand, $|\beta - \beta_c|$ scales well and yields a slope of -0.327 ± 0.01. The expected slope is $-1/3$.

and intercepts C of Table 4. From Eq. (4.38) it is expected that the slopes and C should take the same value for all j, so that the data points would fall on one and the same curve. The difference between the results obtained by using N and N_v should asymptotically decrease as the lattice size goes to infinity. (In the table, n denotes the number of points included in the fit.)

The scaling relation Eq. (2.19) predicts the angle that the trajectories of the zeros will form with respect to the $\mathrm{Re}(K)$ axis as H is varied for large L. In our case the angle is expected to be

$$\psi = \frac{\pi}{2\beta\delta} = 36^\circ . \tag{4.40}$$

This prediction is valid for large system sizes L and small magnetic field. In Fig. 7a we show the trajectories of the first Fisher zero for $N = 4, 6, 8, \ldots, 14$ and magnetic fields in the interval $-0.2 < H < 0.2$. As expected from Eq. (2.19), $H = 0$

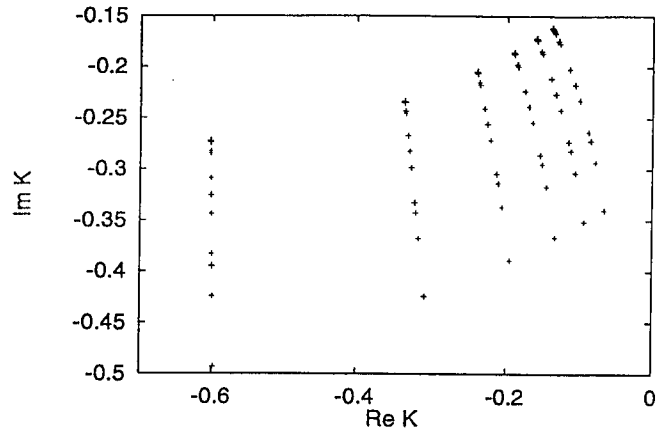

(a)

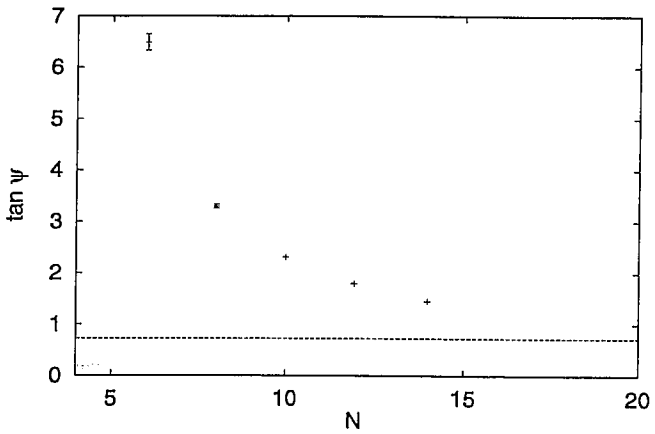

(b)

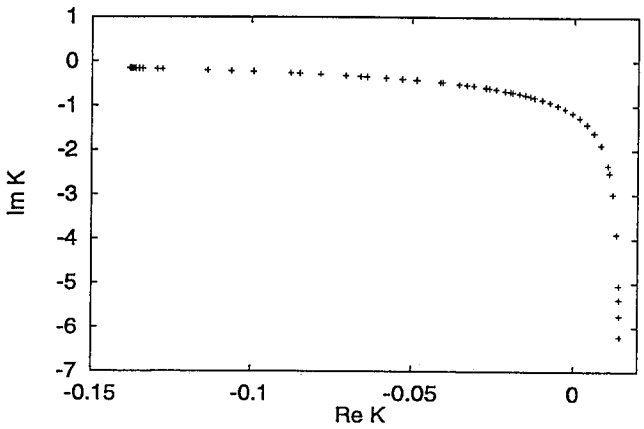

(c)

Fig. 7. (a) Trajectories of the first Fisher zero in the complex K-plane for nonzero magnetic field $-0.2 < \mathrm{Im}(H) < 0.2$. The trajectories are for small square lattices of size $N = 4, 6, 8, 10, 12, 14$ in order from left to right. The angle ψ that the trajectories form with the $\mathrm{Re}(K)$ axis is expected to approach $\psi = \pi/(2\beta\delta) = 36°$ as $N \to \infty$. (b) $\tan\psi$ vs N for small lattices. The dashed line corresponds to the expected asymptotic value of $\tan\psi$ for large N. (c) Breakdown of scaling for strong magnetic field (up to $|H| \approx 2.6$). The angle ψ changes drastically for strong H.

corresponds to the "turning point" closest to the Re(K) axis. Figure 7b and Table 5 show the corresponding values of $\tan\psi$, calculated from fits in the small H range $-0.03 < H < 0.02$. Although ψ does not reach its infinite volume value, Fig. 7b shows the approach to it with increasing lattice size. The breakdown of scaling for very strong H can be observed in Fig. 7c where a trajectory for $|H|$ between zero and 2.6 are shown.

Table 5. Measured ($N = 6, 8, \ldots, 14$) and expected (Eq. (4.40)) slopes of trajectories of zeros in the complex K-plane as the magnetic field H is varied, as a function of the size of the lattice.

N	$\tan\psi \pm \Delta\tan\psi$
6	6.489 ± 0.162
8	3.295 ± 0.036
10	2.308 ± 0.001
12	1.792 ± 0.006
14	1.450 ± 0.002
∞	0.727

We also checked the validity of the scaling relation given by Eq. (2.21). Taking K real, we plotted $H_j(N/j)^{5/6}$ vs $(\beta-\beta_c)(N/j)^{1/3}$. The scaling function F is shown in Fig. 8. All zeros of order $j > 1$ for lattice sizes ($10 \leq N \leq 14$) are included in the same graph. We observe that there exists a range of β in the hot phase where the data points lie approximately on a universal curve defining the function F.

By varying the value of the exponent $-\delta/(\delta+1) = -5/6$ of the scaling variable $\lambda = j/N$ on the y-axis away from its KPZ value, we observed a broadening of

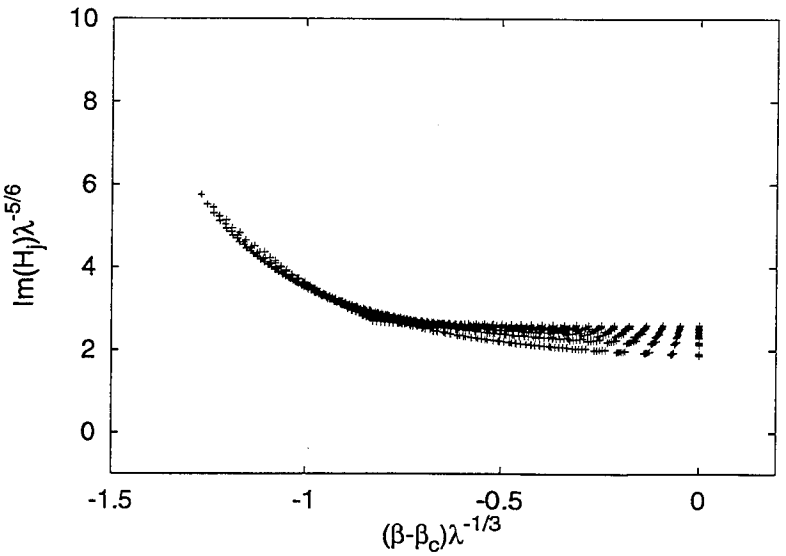

Fig. 8. Check of the scaling relation for the jth Lee–Yang zero $H_j^2\lambda^{-2\delta/(\delta+1)} = F(K\lambda^{-1/(\nu d_H)})$, where $\lambda = j/N$ and F is a universal function. All values of $j > 1$ for lattice sizes in the range $10 \leq N \leq 14$ have been plotted on the same graph. The points are expected to fall on the same universal curve for *large* j.

the curve and in this way we obtained a (somewhat subjective) determination of the exponent combinations

$$\frac{\delta}{\delta+1} = \frac{\beta\delta}{\nu d_{\mathrm{H}}} \approx 0.85 \pm 0.05\,, \tag{4.41}$$

(the equality of these follow from the general exponent equalities and was used in the derivation of the scaling relation (2.21)). This is in excellent agreement with the KPZ value of 5/6.

4.2. *Zeros determined from multihistogramming*

In this section we describe the scaling of the zeros determined numerically from Monte–Carlo data. The lattice sizes investigated here range from 32 to 256 vertices (60–508 triangles). We were able to determine the first five Lee–Yang zeros for the biggest lattice size, while for the smaller ones at most three zeros were visible. For the Fisher zeros, only the zero closest to the real axis was observed for any lattice size.

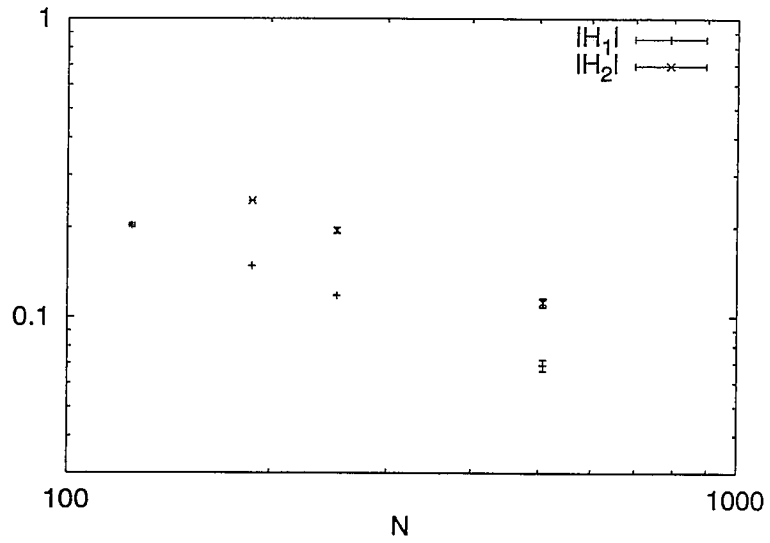

Fig. 9. The first ($j = 1$) and second ($j = 2$) Lee–Yang zeros observed using multihistogramming on dynamical triangular lattices in the size range $64 \leq N_v \leq 256$ ($124 \leq N \leq 508$). The slopes of the lines should be given by $-\beta\delta/(\nu d_{\mathrm{H}}) = -5/6$.

The Lee–Yang zeros we observed with multihistogramming are listed in Table 1 (Fig. 9). The least-squares fits to Eq. (4.35) give for the first and second Lee–Yang zeros,

$$\frac{\beta\delta}{\nu d_{\mathrm{H}}} = 0.773 \pm 0.013 \quad (j = 1)\,, \tag{4.42}$$

$$\frac{\beta\delta}{\nu d_{\mathrm{H}}} = 0.788 \pm 0.033 \quad (j = 2)\,. \tag{4.43}$$

All data points with $j \leq 2$ shown in Table 1 were included in the fits. Using N_v instead of N for the volume of the system we obtain:

$$\frac{\beta\delta}{\nu d_{\mathrm{H}}} = 0.787 \pm 0.013 \quad (j = 1)\,, \tag{4.44}$$

$$\frac{\beta\delta}{\nu d_{\mathrm{H}}} = 0.800 \pm 0.034 \quad (j = 2)\,, \tag{4.45}$$

which gives a measure of the presence of finite size effects. The results are in quite good agreement with the expected value of $\beta\delta/\nu d_{\mathrm{H}} = 5/6$. From the exactly known value $\nu d_{\mathrm{H}} = 3$ we obtain

$$\beta\delta = 2.36 \pm 0.04 \quad (j = 1)\,, \tag{4.46}$$

$$\beta\delta = 2.40 \pm 0.10 \quad (j = 2)\,. \tag{4.47}$$

The exact value of this combination of exponents is 2.5.

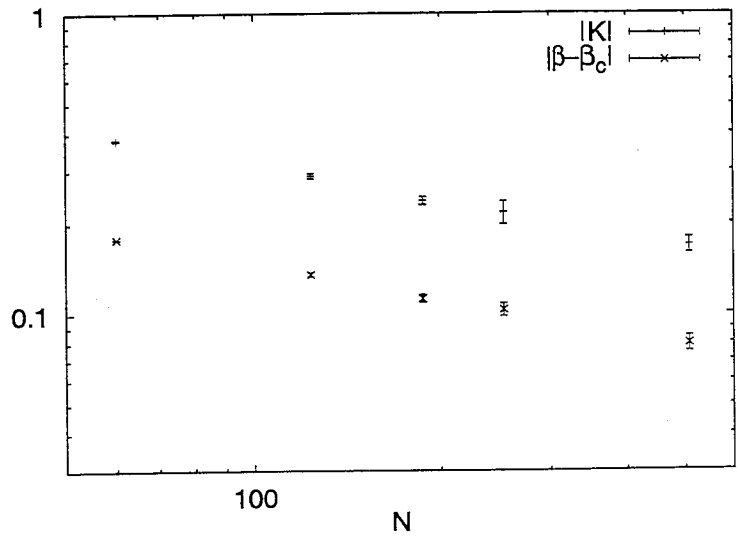

Fig. 10. The first Fisher zero observed using multihistogramming on dynamical triangular lattices in the size range $32 \leq N_v \leq 256$ ($60 \leq N \leq 508$). The slopes of the lines are expected to be $-1/(\nu d_{\mathrm{H}}) = -1/3$.

The value of νd_{H} extracted from Eq. (4.37) is somewhat lower than three, but still remarkably close to it given the small size of the systems considered. The plot of the observed zeros is shown in Fig. 10 ($\ln|K|$ resp. $\ln|\beta - \beta_{\mathrm{c}}|$ vs $\ln(N)$). We also calculated the slope of $\ln|K|$ vs $\ln(N_v)$ and of $\ln|\beta - \beta_{\mathrm{c}}|$ vs $\ln(N_v)$. The results are shown in Table 6. We note that by discarding the smallest lattices the value of νd_{H} approaches 3, albeit with an increasing error. For example, including only the three largest lattices we obtain (using N for volume):

$$\frac{1}{\nu d_{\mathrm{H}}} = 0.350 \pm 0.067\,. \tag{4.48}$$

Table 6. Finite size scaling for the first Fisher zero.

Quantity fitted	$1/(\nu d_{\mathrm{H}})$
$\ln\lvert K\rvert$ vs $\ln(N)$	0.392 ± 0.016
$\ln\lvert K\rvert$ vs $\ln(N_v)$	0.407 ± 0.017
$\ln\lvert\beta - \beta_{\mathrm{c}}\rvert$ vs $\ln(N)$	0.386 ± 0.014
$\ln\lvert\beta - \beta_{\mathrm{c}}\rvert$ vs $\ln(N_v)$	0.401 ± 0.014

5. Conclusion

We have computed the positions of the singularities of the partition function for the two-dimensional Ising model coupled to gravity in the complex plane. Both Lee–Yang and Fisher zeros were studied.

We verified the result in Ref. 12 that the Lee–Yang zeros are located on the unit circle of the complex fugacity plane. This presents us with the challenge of proving a corresponding Lee–Yang theorem for the case when a fluctuating metric contributes an additional quantum degree of freedom. We also observed that the Fisher zeros form one-dimensional curves in the complex temperature plane.

Given the small size of the systems we studied, we obtained reasonable agreement with scaling laws derived from ordinary renormalization group arguments. Although one cannot use our results to accurately determine the scaling exponents, the extracted exponent combinations show a reasonable agreement with their exactly known values.[11] This, together with the fact that a diverging matter correlation length exists in the system,[13] gives us confidence to conclude that the critical behaviour of the system is given by the scaling of the distribution of the complex zeros of the partition function.

References

1. C. N. Yang and T. D. Lee, *Phys. Rev.* **87**, 404; 410 (1952).
2. M. Fisher, in *Lectures in Theoretical Physics* **VIIC** (University of Colorado Press, 1965).
3. V. Matveev and R. Shrock, *Phys. Rev.* **E53**, 254 (1996); *Phys. Lett.* **A215**, 271 (1996).
4. R. Abe, *Prog. Theor. Phys.* **37**, 1070 (1967); **38**, 72; 568 (1967).
5. S. Ono, Y. Karaki, M. Suzuki and C. Kawabata, *J. Phys. Soc. Japan* **25**, 54 (1968).
6. C. Itzykson, R. B. Pearson and J. B. Zuber, *Nucl. Phys.* **B220**, 415 (1983).
7. M. E. Fisher, *Phys. Rev. Lett.* **40**, 1610 (1978); P. J. Kortman and R. B. Griffiths, *ibid.* **27**, 1439 (1971).
8. P. H. Damgaard and U. Heller, *Nucl. Phys.* **B410**, 494 (1993).
9. V. Knizhnik, A. Polyakov and A. Zamolodchikov, *Mod. Phys. Lett.* **A3**, 819 (1988).
10. V. A. Kazakov, *Phys. Lett.* **A119**, 140 (1986).
11. D. V. Boulatov and V. A. Kazakov, *Phys. Lett.* **B186**, 379 (1987).
12. M. Staudacher, *Nucl. Phys.* **B336**, 349 (1990).
13. J. Ambjørn, K. N. Anagnostopoulos, U. Magnea and G. Thorleifsson, *Phys. Lett.* **B388**, 713 (1996); J. Ambjørn and K. N. Anagnostopoulos, "Quantum geometry of 2D gravity coupled to unitary matter", NBI-HE-96-69 (hep–lat/9701006).

14. D. A. Johnston, *Phys. Lett.* **B314**, 69 (1993); C. F. Baillie and D. A. Johnston, *ibid.* **B357**, 287 (1995).
15. M. G. Harris and J. Ambjørn, *Nucl. Phys.* **B474**, 575 (1996).
16. M. Falcioni, E. Marinari, M. L. Paciello, G. Parisi and B. Taglienti, *Phys. Lett.* **B102**, 270 (1981).
17. M. Falcioni, E. Marinari, M. L. Paciello, G. Parisi and B. Taglienti, *Phys. Lett.* **B108**, 331 (1982); E. Marinari, *Nucl. Phys.* **B235**, 123 (1984).
18. J. Jurkiewicz, A. Krzywicki, B. Petersson and B. Söderberg, *Phys. Lett.* **B213**, 511 (1988); C. F. Baillie and D. A. Johnston, *ibid.* **B286**, 44 (1992); S. Catterall, J. Kogut and R. Renken, *ibid.* **B292**, 277 (1992); J. Ambjørn, B. Durhuus, T. Jonsson and G. Thorleifsson, *Nucl. Phys.* **B398**, 568 (1993).
19. J. Ambjørn, G. Thorleifsson and M. Wexler, *Nucl. Phys.* **B439**, 187 (1995).
20. A. M. Ferrenberg and R. H. Swendsen, *Phys. Rev. Lett.* **61**, 2635 (1988).
21. N. A. Alves, B. A. Berg and R. Villanova, *Phys. Rev.* **B41**, 383; **B43**, 5846 (1991).
22. K. N. Anagnostopoulos, M. J. Bowick and E. Marinari, unpublished.
23. S. Catterall, G. Thorleifsson, M. Bowick and V. John, *Phys. Lett.* **B354**, 58 (1995).
24. J. Ambjørn, J. Jurkiewicz and Y. Watabiki, *Nucl. Phys.* **B454**, 313 (1995).
25. J. Ambjørn and Y. Watabiki, *Nucl. Phys.* **B445**, 129 (1995).
26. D. Dhar, *Phys. Rev. Lett.* **51**, 853 (1983); J. L. Cardy, *ibid.* **54**, 1354 (1985).
27. B. Derrida, L. De Seze and C. Itzykson, *J. Stat. Phys.* **33**, 559 (1983).
28. W. van Saarlos and D. Kurtze, *J. Phys.* **A17**, 1301 (1984); J. Stephenson and R. Couzens, *Physica* **A129**, 201 (1984).
29. V. Matveev and R. Shrock, *J. Phys.* **A28**, 5235 (1995).
30. P. H. Damgaard and J. Lacki, *Int. J. Mod. Phys.* **C6**, 819 (1995).
31. M. Baake, U. Grimm and C. Pisani, *J. Stat. Phys.* **78**, 285 (1995).
32. S. Huang, K. J. M. Moriarty, E. Myers and J. Potvin, *Z. Phys.* **C50**, 221 (1991).
33. G. K. Savvidy and N. G. Ter-Arutyunyan Savvidy, EPI-865-16-86 (1986); *J. Comput. Phys.* **97**, 566 (1991); N. Z. Akopov, G. K. Savvidy and N. G. Ter-Arutyunyan Savvidy, *ibid.* **97**, 573 (1991).
34. M. Lüscher, *Comput. Phys. Commun.* **79**, 100 (1994); F. James, *ibid.* **79**, 111 (1994); **97**, 357(E) (1996).